Influence of Wall Boundary Condition on the Dynamics of Premixed Flames Propagating in a Closed Channel

Xiaoxi Li, Huahua Xiao, Jinhua Sun
State Key Laboratory of Fire Science, University of Science and Technology of China
Hefei, Anhui Province, P.R. China

1 Introduction

Understanding the dynamics of unsteady flame propagation in confined regions is important for explosion safety and combustion applications. Premixed flame propagation in a tube or channel is generally very complex and can undergo various shape changes, such as tulip and distorted tulip flames [1-6]. Ellis [7] published the first photograph of the tulip flame in 1928. Since then, a large number of studies have been conducted to explain the characteristics and mechanism of tulip flame formation . Several explanations were put forward, including Landau–Darrieus instability [8], Rayleigh-Taylor instabilities [9], pressure effects [10], and interaction between flame front and flame-induced flow [11, 12]. Till now, there is still no decisive conclusion or single recognized interpretation about the mechanism of tulip flame formation.

A new phenomena of premixed flame dynamics, the distorted tulip flame (DTF), was discovered by Xiao et al. [1] in the experiments of premixed hydrogen-air flame propagation. In general, a distorted tulip flame is formed after the formation of tulip flame. It was found that the formation of a distorted tulip flame is closely connected with pressure waves. Numerical simulation and theoretical analysis demonstrated that Rayleigh–Taylor instability driven by pressure waves is the primary cause of the formation of distorted tulip flame [5, 6].

Although wall boundary condition may play an important role in flame propagation in tubes, its effect on the flame dynamics has not been fully understood, especially for distorted tulip flames. Gonzalez et al. [8] suggested that wall friction was not important for tulip flame formation. The numerical simulation of Xiao et al. [13] supports this conclusion and implies that wall friction may not be important for the formation of distorted tulip flame either. Marra and Continillo [14], however, argued that wall friction can be the determining cause for the formation of a tulip flame. Lee and Tsai [15] found through numerical simulations that the flame in a tube with adiabatic walls evolves differently than that with isothermal walls. The work by Kim et al. [16] also indicates that both the propagation velocity and structure of a flame change noticeably under different wall boundary conditions.

This paper presents simulations of flame dynamics in a tube under three different types of wall boundary conditions: adiabatic free-slip wall, adiabatic no-slip wall and isothermal wall. Two-dimensional reactive

Correspondence to: Huahua Xiao, xiaoh@ustc.edu.cn

Navier-Stokes equations are solved with high-order algorithms and adaptive mesh refinement (AMR). The objective of this work is to interpret the effect of wall boundary condition on the flame dynamics, especially the formation and evolution of distorted tulip flame. Generation and characteristics of pressure waves and their interactions with flame front will be examined in detail in the presentation.

2 Physical and Numerical Models

The governing equations, which can be found in [5], are the two-dimensional fully-compressible reactive Navier-Stokes equations with conservations of mass, energy and species. A single-step chemical-diffusive model is used to model the chemical reaction and energy release of a stoichiometric mixture of hydrogen and air. The reaction rate $\dot{\omega}$, is defined using the Arrhenius equation:

$$\dot{\omega} = dY/dt = A\rho Y exp\left(-\frac{Ea}{RT}\right), \quad (1)$$

where, Y, t, T, A, ρ, Ea and R are the unburned mass friction, time, temperature, pre-exponential factor, density, activation energy, and universal gas constant, respectively. The modeling parameters are in [5]. The convection terms are solved using a fifth-order MUSCL scheme with HLLC fluxes [17]. The third-order Runge–Kutta method is used for time integration.

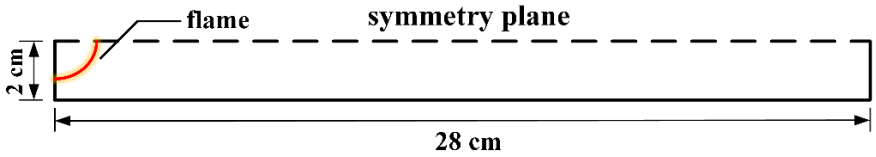

Figure 1. Computational domain.

The 2D computational domain is a 4 cm × 28 cm channel, as shown in Figure 1. The wall boundary conditions are varied in the calculations as adiabatic free-slip, adiabatic no-slip and isothermal. The adaptive mesh refinement (AMR) with the Paramesh library [18] provides a dynamically adapting mesh that helps resolve important flow features such as boundary layers, pressure waves, and reaction fronts. The smallest cell size is 15.625 μm, corresponding to 22 computational cells in the flame at initial conditions, which was shown to be adequate to simulate flame propagation in the configuration considered [5]. It also showed that a maximum grid size of 1/40 cm is sufficient for the present calculations. The simulated ignition source is a small circular combustion gas with 1mm radius at the left end on the tube axis. The incipient pressure and temperature are 1 atm and 293 K, respectively.

3 Results and discussion

Figure 2 shows the evolution of premixed hydrogen-air flame in the channel as a function of time with (a) adiabatic no-slip boundary, (b) adiabatic free-slip boundary, and (c) isothermal boundary conditions. The result shows that the flame front experiences similar flame changes in the early stages under three different wall boundary conditions. That is the flame evolves from a semi-circular flame, to a finger-shaped flame, to a tulip flame, and then to a distorted tulip flame. Nonetheless, the flame evolution becomes significantly different between different boundary conditions after the formation of distorted tulip flame. In the simulation with adiabatic no-slip boundary conditions, a secondary distorted tulip flame forms before the disappearance of the first distorted tulip flame as the flame continues to propagate, as shown at 5.55 ms in

Fig. 2a. A series of distorted tulip flames is produced one after another until the end of combustion, as detailed in [5, 6]. In the case with adiabatic free-slip boundary conditions, the distorted tulip flame is flattened out to form a nearly planar flame, as shown at 5.31 ms in Fig. 2b, instead of producing a second distorted tulip shape. Then a noticeably corrugated flame is formed, as shown at 6.65 ms in Fig. 2b. The flame develops a flattened surface again (see 7.9 ms) and subsequently another corrugated shape (12.45 ms in Fig. 2b). In fact, this process is repeated in the rest of the flame propagation and the wrinkles on the corrugated flame surface gradually become smaller. In the case with isothermal boundary conditions, a second distorted tulip flame forms at about 5.75 ms (Fig. 2c). However, the flame surface flattens out, as shown at 7.57 ms. After that, a noticeably corrugated flame is produced, as shown at 8.63 ms. This process is repeated for several times. At the final flame stage, the flame develops a tulip shape again, as shown at 14.18 ms in Fig. 2c.

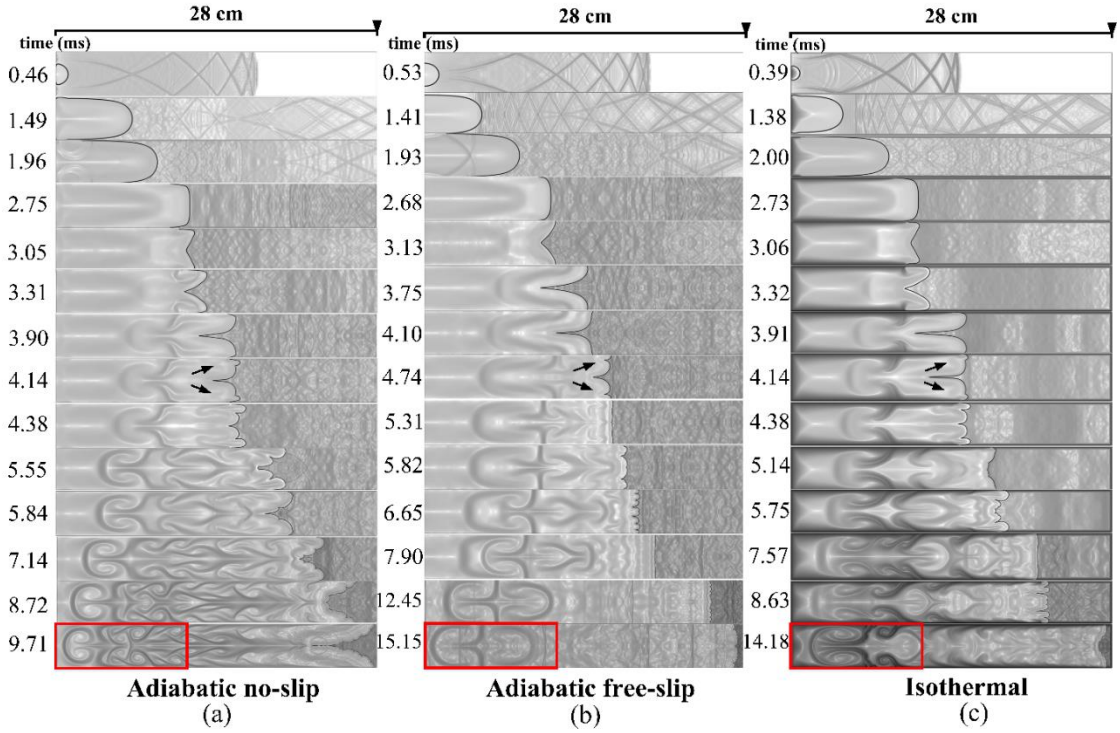

Figure 2. Sequences of schlieren fields of flame propagating in tubes under three different wall boundary conditions: (a) adiabatic no-slip wall, (b) adiabatic free-slip wall and (c) isothermal wall. The pictures show the approximate corresponding propagation phases of three wall boundary conditions.

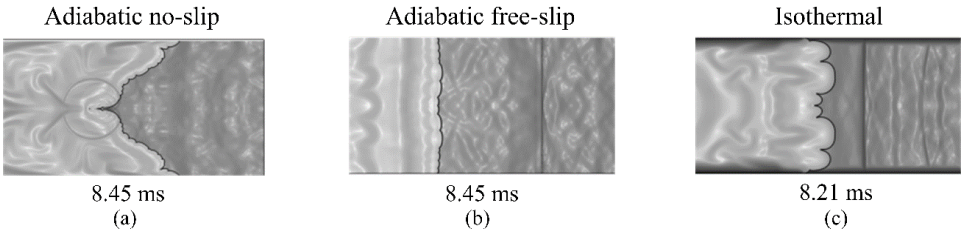

Figure 3. Comparison of the pressure waves generated during flame propagation under three different wall boundary conditions.

There are also significant differences in the vortex motion during the formation and evolution of DTFs under three boundary conditions. The dark spots (indicated by arrows at 4.14 ms in Fig. 2a, 2c and 4.74ms in Fig. 2b) behind the flame front are the motion of vortices in the burned gas which are created when the DTF forms. At the early stage of DTF, such vortices in the burned gas are similar for different boundary conditions. Nevertheless, obvious discrepancy can be seen when the vortices travel further into the burned region. In the later stage of flame propagation, the leading vortex under different boundary conditions all takes the appearance of a mushroom structure (see Fig. 2 marked with red box), but different in the details. The mushroom structure in the case of isothermal boundary condition has a similar contour as the one under adiabatic free-slip boundary condition, but more complex. As the flame front approaches the right end wall of the channel, the whole leading vortex moves closer to the left end wall for all the cases considered.

The differences in the flame shape and vortex motion are closely related to the different combustion generated waves under different wall boundary conditions. Noticeable shock waves are generated by coalescing compression waves in the later flame stage under adiabatic free-slip and isothermal boundary conditions, for example, at 8.45 and 8.21 ms in Fig. 3b and 3c, respectively. The interaction between the shock waves and flame front can lead to Rictmyer-Meshkov (RM) instabilities that change the dynamics of the flame. The RM instabilities are more evident with isothermal boundary because the shock wave is stronger in this case, as shown at 8.63 ms in Fig. 2c. In contrast, in the case with adiabatic no-slip boundary condition, only compression waves are generated without any shock waves in the entire process of flame propagation. Hence, the wall boundary condition has a significant effect on the pressure wave generation and consequently the dynamics of distorted tulip flame.

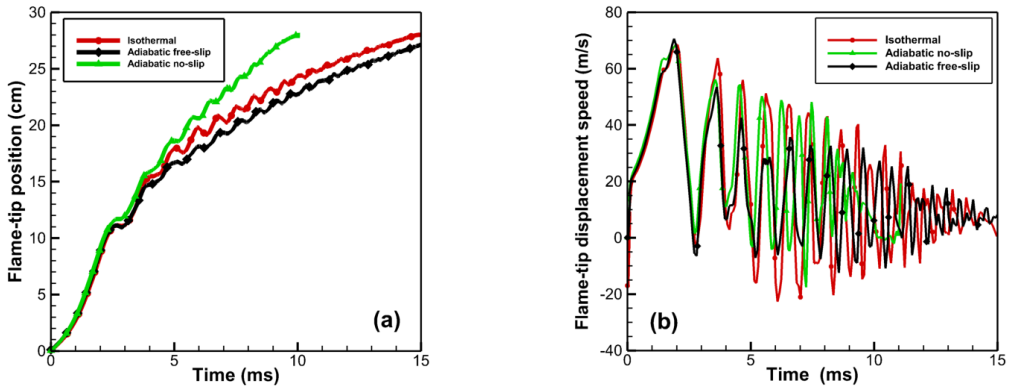

Figure 4. Time tracks of (a) position and (b) displacement speed of flame-tip under three wall boundary conditions.

Figure 4 presents the comparison of (a) position and (b) propagation speed of the flame under different boundary conditions. In the early stages, the influence of boundary condition on flame speed is insignificant since the flame does not reach the walls. That is the reason for the similar growth in the flame-tip position and average flame displacement speed under three different boundary conditions before 2.5 ms. The contact of flame with channel sidewalls causes a sudden loss of flame area and thus an abrupt decrease in the displacement speed of flame-tip. Pressure waves are generated in this process and the oscillations in flame propagation result from interaction of flame with pressure waves, as demonstrated in the previous work [5, 6]. In the later stages of flame propagation, adiabatic no-slip and isothermal boundary conditions have a higher flame propagation speed than that under the adiabatic free-slip condition. Then, the amplitude of the flame oscillation begins to show obvious differences. Noticeably, isothermal condition shows greater amplitude of oscillation for most of the time in the later flame stage. This is closely related to the differences in the strength of strong shock waves generated under different boundaries (discussed below).

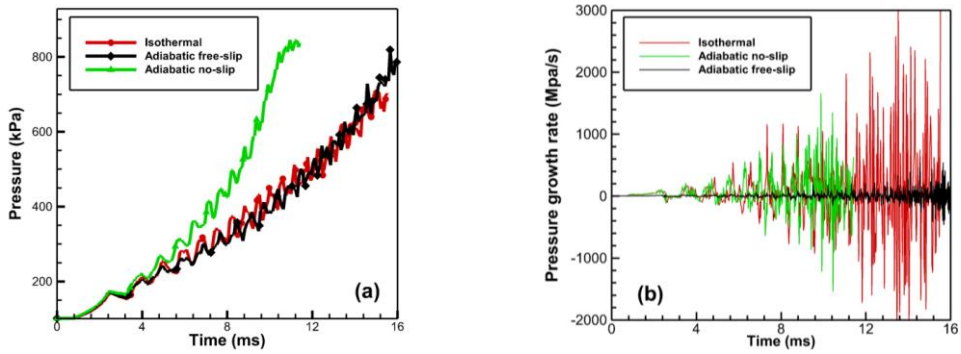

Figure 5. Time tracks of (a) pressure and (b) pressure growth rate under three boundary conditions.

Figure 5 shows the comparison of (a) pressure and (b) pressure growth rate as a function of time recorded at the right end wall of the tube on the axis. Primary pressure waves, demonstrated to be expansion waves, are generated due to sudden loss of flame surface area when the lateral flame front touches the channel side walls [5]. The pressure and its growth rate increase similarly under three different boundary conditions in the early stages. Significant differences occur in the later stages. The pressure in the case of adiabatic no-slip boundary increases steeply, and its pressure growth rate is greater than the other two cases when approaching the right end of the tube, as shown in Fig. 5a and 5b. The pressure with the case of adiabatic free-slip and isothermal conditions competitively increases. The pressure of adiabatic free-slip boundary condition in the final stage is greater than that of isothermal boundary condition.

There are significant differences in the pressure growth rate under three boundary conditions, as shown in Fig. 5b. The pressure growth rate under adiabatic no-slip boundary condition shows strong oscillations until the flame approaching the right end wall at about 11.5 ms. The pressure growth rate of adiabatic free-slip boundary condition shows uniform and relatively smaller amplitude oscillations from beginning to end. The isothermal boundary condition leads more drastic oscillations in the pressure growth rate in the later stages. The amplitude of oscillations in pressure growth rate is much larger than those in the cases with the other two conditions, as shown in Fig. 5b. That means stronger shock waves are generated with isothermal walls. The difference in the pressure growth rate or the pressure wave strength lies in the difference in the loss of flame surface and heat when the flame touches the channel sidewalls. The loss of flame surface in the adiabatic free-slip case is smaller and thus weaker expansion waves are generated than the adiabatic no-slip case. The contact of flame with the sidewalls results in heat losses and flame quenching in addition to reduction of flame surface in the isothermal case, and consequently leads to stronger pressure waves.

The results of the effect of wall boundary condition on the strength of pressure waves generated and oscillating flame behavior provide further evidence of the importance of pressure waves on the dynamics of distorted tulip flame. The amplitude of the pressure oscillation increases very quickly when the flame approaches the right end. This implies that pressure waves are significantly amplified at the later stages of the burning process. And there is significant discrepancy in the amplification extent under different boundary conditions. The stronger shock wave under isothermal boundary condition leads to greater amplitude of oscillation in the later stage. Thus we see that wall boundary condition has great effect on the generation and characteristics of pressure waves which are responsible for distorted tulip flame formation.

Acknowledgments

This study was supported by University of Science and Technology of China through the Thousand Talent Program for Young Outstanding Scientists.

References

[1] Xiao H, et al. (2012). Experimental and numerical investigation of premixed flame propagation with distorted tulip shape in a closed duct. Combust. Flame. 159: 1523.

[2] Matalon M, Metzener P. (1997). The propagation of premixed flames in closed tubes. J. Fluid Mech. 336: 331.

[3] Dunn-Rankin D, Sawyer RF. (1998). Tulip flames: changes in shape of premixed flames propagating in closed tubes. Exp. Fluids. 24: 130.

[4] Bychkov V, et al. (2007). Flame acceleration in the early stages of burning in tubes. Combust. Flame. 150: 263.

[5] Xiao H, Houim RW, Oran ES. (2015). Formation and evolution of distorted tulip flames. Combust. Flame. 162: 4084.

[6] Xiao H, Houim RW, Oran ES. (2017). Effects of pressure waves on the stability of flames propagating in tubes. Proc. Combust. Inst. 36: 1577.

[7] Ellis OCdC. (1928). Flame movement in gaseous explosive mixtures. J. Fuel Sci. 7: 502.

[8] Gonzalez M, Borghi R, Saouab A. (1992). Interaction of a flame front with its self-generated flow in an enclosure: The “tulip flame” phenomenon. Combust. Flame. 88: 201.

[9] Clanet C, Searby G. (1996). On the "tulip flame" phenomenon. Combust. Flame. 105: 225.

[10] GuÉNoche H. (1964). Flame propagation in tubes and in closed vessels. AGARDograph. 75: 107.

[11] Najim YM, Mueller N, Wichman IS. (2015). On premixed flame propagation in a curved constant volume channel. Combust. Flame. 162: 3980.

[12] Ponizy B, Claverie A, Veyssière B. (2014). Tulip flame - the mechanism of flame front inversion. Combust. Flame. 161: 3051.

[13] Xiao H, Sun J, Chen P. (2014). Experimental and numerical study of premixed hydrogen/air flame propagating in a combustion chamber. J. Hazard. Mater. 268: 132.

[14] Marra FS, Continillo G. (1996). Numerical study of premixed laminar flame propagation in a closed tube with a full navier-stokes approach. Symp. (Int.) on Combust. 26: 907.

[15] Lee ST, Tsai CH. (1994). Numerical investigation of steady laminar flame propagation in a circular tube. Combust. Flame. 99: 484.

[16] Kim NI, Maruta K. (2006). A numerical study on propagation of premixed flames in small tubes. Combust. Flame. 146: 283.

[17] Thornber B, et al. (2008). An improved reconstruction method for compressible flows with low Mach number features. J. Comput. Phys. 227: 4873.

[18] MacNeice P, et al. (2000). PARAMESH: A parallel adaptive mesh refinement community toolkit. CoPhC. 126: 330.